1521-0103/371/3/583–589$35.00
THE JOURNAL OF PHARMACOLOGY AND EXPERIMENTAL THERAPEUTICS

https://doi.org/10.1124/jpet.119.259135
J Pharmacol Exp Ther 371:583–589, December 2019

The Journal of PHARMACOLOGY And Experimental Therapeutics

Utilization of ^{18}F-Fluorodeoxyglucose–Positron Emission Tomography To Understand the Mechanism of Nicotinamide Phosphoribosyltransferase Inhibitors In Vivo[S]

Sarah R. Mudd, Martin J. Voorbach, Dong Cheng, Min Cheng, Jun Guo, Wenqing Gao, Fritz G. Buchanan, Chris Tse, and Julie Wilsbacher

Abbvie, North Chicago, Illinois

Received April 23, 2019; accepted September 23, 2019

ABSTRACT

Cancer cells are highly dependent on NAD^+/NADH produced via the nicotinamide salvage pathway. The rate-limiting enzyme in this pathway is the nicotinamide phosphoribosyltransferase (NAMPT), which we have targeted with novel NAMPT inhibitors. NAMPT inhibition elicits depletion of total cellular NAD^+ levels and ultimately cytotoxicity via depletion of cellular ATP levels. ^{18}F-fluorodeoxyglucose– positron emission tomography (FDG-PET) is a translational imaging tool to assess glucose utilization in tumors and normal tissue. We used FDG-PET to understand the timing of ATP depletion in vivo and better understand the pharmacology of NAMPT inhibitors. Because of the intimate relationship between cellular ATP levels and cell viability, we developed an in-depth understanding of our NAMPT inhibitor pharmacology and the relationship with changes in tumor FDG uptake. Taken together, we show that FDG-PET could be used as a biomarker in clinical studies to understand dose and provide proof of mechanism for NAMPT inhibitors.

SIGNIFICANCE STATEMENT

Our imaging data suggest that tumor ^{18}F-fluorodeoxyglucose uptake can provide insight into the ATP status inside the tumor after nicotinamide phosphoribosyltransferase (NAMPT) therapy, with a novel NAMPT inhibitor. Such an approach could be used clinically as a pharmacodynamic biomarker to help understand the implications of dose, schedule, rescue strategy, or other clinical biomarkers.

Introduction

^{18}F-fluorodeoxyglucose (FDG)–positron emission tomography (PET) is an imaging technique that utilizes FDG, a glucose analog, as a tracer for PET. FDG-PET is a common nuclear medicine imaging technique in oncology that is typically used for diagnosis, staging disease, and monitoring treatment response. FDG uptake has been correlated to glucose transport into the cell, which requires ATP. After intravenous injection, FDG is transported into cells depending on the metabolic needs of the cell. Once FDG is internalized by transporters, it is phosphorylated by hexokinase, but cannot be further used because the C-2 hydroxyl group has been replaced by F-18.

Cancer cells exhibit an altered metabolism that has been referred to as the Warburg effect (Chiarugi et al., 2012). This altered metabolism is characterized by the excess catabolism of glucose for glycolysis that requires NAD^+/NADH-dependent REDOX reactions. Additionally, persistent DNA damage in cancer cells leads to activation of repair enzymes, including the NAD^+-dependent poly(ADP)-ribose polymerases, which consume NAD^+ and produce nicotinamide (NM) as a byproduct (Gupte et al., 2017). There is a greater demand on cancer cells to recycle NM to NAD^+ to support the high level of poly(ADP)-ribose polymerase activity. Nicotinamide phosphoribosyltransferase (NAMPT) is the rate-limiting enzyme for the salvage of NAD^+ using NM as a biosynthetic precursor (Imai, 2009; Burgos, 2011; Sampath et al., 2015). The Preiss–Handler pathway is another NAD^+ biosynthetic pathway that utilizes dietary nicotinic acid (NA) via NA phosphoribosyltransferase (NAPRT) (Preiss and Handler, 1958). The NAPRT1 gene is epigenetically silenced in a significant percentage of cancers, providing an opportunity to select patients whose cancers are dependent on NAMPT to regenerate NAD^+ (Shames et al., 2013; Duarte-Pereira et al., 2016). NAPRT1 is expressed on normal tissues, which would allow for NAD^+ production from dietary NA and potentially mitigate toxicity of NAMPT inhibitors in patients with NAPRT1-deficient tumors. Given the increased reliance on regenerating NAD^+ from NM via the NAMPT pathway in cancer cells, inhibition of NAMPT represents a point of therapeutic intervention to target cancer cells.

Inhibitors of NAMPT have been investigated as anticancer agents and elicit cytotoxicity via depletion of total cellular

All authors are employees of AbbVie. The design, study conduct, and financial support for this research were provided by AbbVie.
https://doi.org/10.1124/jpet.119.259135.
[S] This article has supplemental material available at jpet.aspetjournals.org.

ABBREVIATIONS: CT, computed tomography; FDG, fluorodeoxyglucose; NA, nicotinic acid; NADt, NADH + NAD^+; NAMPT, nicotinamide phosphoribosyltransferase; NAPRT, NA phosphoribosyltransferase; NM, nicotinamide; PET, positron emission tomography; SUV, standard uptake value.

NAD^+ levels (Sampath et al., 2015). The mechanism of cytotoxicity is mediated by the sequential of depletion of total NAD levels, then ATP, and subsequently cell death (Wilsbacher et al., 2017). Given the retention of FDG in cells requires the ATP-dependent phosphorylation by hexokinase, the ability of FDG-PET to serve as a downstream pharmacodynamic marker of NAMPT inhibitors was investigated based on the following hypothesis: NAMPT inhibition will cause NAD^+ and ATP depletion, which are necessary for glycolysis. As a result, FDG-PET can be used to monitor metabolic changes in the tumor due to NAMPT inhibition.

FDG-PET was performed to provide proof of mechanism and explore the patient selection and toxicity mitigation strategies by imaging FDG-PET response to NAMPT inhibition in cancer models with and without NAPRT1 expression and NA supplementation. We demonstrated that decreases in tumor FDG uptake correspond to decreases in ATP levels. Next, we performed FDG-PET experiments to understand the impact of the Preiss–Handler pathway on NAPRT-deficient and -proficient tumors by codosing NA with the NAMPT inhibitor. The NAMPT inhibitors used in these studies, A-1293201 and A-1326133, have previously been published (Wilsbacher et al., 2017).

Materials and Methods

Tumor Models. AbbVie is committed to the internationally-accepted standard of reduction, refinement, and replacement and adhering to the highest standards of animal welfare in the company's research and development programs. Animal studies were approved by AbbVie's Institutional Animal Care and Use Committee or Ethics Committee. Animal studies were conducted in an Association for Assessment and Accreditation of Laboratory Animal Care–accredited program in which veterinary care and oversight were provided to ensure appropriate animal care.

HCT-116 and A2780 cells were purchased from American Type Culture Collection (Manassas, VA) and European Collection of Authenticated Cell Cultures, respectively. NCI-H460-LM cells are a derivative of NCI-H460 (American Type Culture Collection). All cell lines were cultured in RPMI 1640 (Invitrogen, Carlsbad, CA) plus 10% fetal bovine serum (HyClone, Logan, UT). Cells were maintained at a maximum of 80% confluency and viability greater than 98%.

On the day of inoculation, tumor cells were mixed with 50% Matrigel (BD Biosciences, San Jose, CA), and 0.5×10^6, 1×10^6, and 1×10^6 cells, respectively, per mouse were injected subcutaneously into the right flank of 6- to 8-week-old severe combined immunodeficiency female mice (Charles River Laboratories, Wilmington, MA).

NAMPT Inhibitor Dosing in Mice. Animals were treated with A-1293201, A-1326133, or vehicle (5% ethanol, 5% Tween 80, 20% polyethylene glycol 400, 70% saline) via oral gavage for 3 consecutive days, followed by a 4-day dosing holiday, with the exception of the high-dose NAMPT inhibitor PET experiment in the H460 model in which treatment was given for 4 consecutive days, followed by a 3-day dosing holiday. If NA was given, treatment occurred via oral garage at a dose of 50 mg/kg (0.05% ethanol in sterile water) 30 minutes prior to NAMPT inhibitor treatment. When treatment occurred on an imaging day, FDG was dosed approximately 60 minutes after the NAMPT inhibitor was given.

In Vivo Pharmacodynamic Studies. For the single-dose study, 6- to 8-week-old severe combined immunodeficiency female mice (Charles River Laboratories) bearing HCT116 xenografts were dosed by mouth with A-1293201 at 7.5 or 30 mg/kg. Tumors were collected at 0.5, 1, 6, 24, 48, and 72 hours; snap frozen; and stored at −80°C. For the multiple-dose study, mice bearing HCT116 xenografts were dosed by mouth with A-1293201 at 30 mg/kg once per day for 3 days. Tumors were collected at 6 or 24 hours after each dose. Tumors were pulverized while still frozen and homogenized in NAD^+/NADH extraction buffer (MBL, Woburn, MA). Total protein levels were measured using the Pierce bicinchoninic acid assay kit (Thermo Fisher Scientific, Waltham, MA), and samples were diluted to 1 mg/ml. Total NAD levels (NADt = NADH + NAD^+) were measured using the MBL NAD^+/NADH quantification kit. Data were normalized to total NAD levels in HCT116 tumors from mice that were not dosed with compound.

In Vitro Pharmacodynamic Studies. HCT116 and H460-LM cells were treated with DMSO or different doses of A-1293201. At 6, 24, 48, and 72 hours after compound was added, cells were harvested for NADt and ATP measurements. Cells in the NADt plates were washed with PBS and stored at −80°C until the end of the time course. Plates were then thawed, and 50 μl PBS was added to each well. NADt levels were measured using the Promega NAD^+/NADH Glo assay. ATP levels were measured using the Promega Cell Titer Glo assay (Promega, Madison, WI). Data were normalized to NADt and ATP levels in cells treated with DMSO.

In Vivo Efficacy Studies. The tumors were allowed to grow to a predetermined size, at which time mice were allocated by tumor volume into study groups, so that the mean tumor volumes of the groups were comparable. Mice were then entered into the dosing phase of the study (described below). Tumor volumes were recorded, and imaging data were collected according to the design of the study. Tumor volumes were estimated by the formula $V = (L \times W^2)/2$, where $L > W$ and V is the volume (cubic millimeters), L is the tumor length (millimeters), and W is the tumor width (millimeters), measured at right angles using a digital caliper.

PET/Computed Tomography Imaging and Analysis. Animals undergoing FDG-PET imaging were fasted for at least 8 hours prior to FDG injection. Animals were maintained at 37°C throughout the imaging session. Mice were anesthetized using 2% isoflurane during PET/CT imaging. Images were acquired on an Inveon micro-PET/CT scanner (Siemens, Knoxville, TN). FDG (IBA Molecular, Dulles, VA) (200 μCi in 100–200 μl) was injected via tail vein, and animals were imaged approximately 60 minutes postinjection. Three animals were imaged at once using a modified Minerve bed (Bioscan, Washington, DC). Computed tomography (CT) scans were acquired at 80 kVp, 500 μAs, and 180 rotation steps over 360°. PET images were acquired for 7 minutes. The study designs are represented in Supplemental Fig. 1 for the different FDG-PET experiments. In the experiment for Fig. 3 (Supplemental Fig. 1A), animals were divided into two groups to minimize the adverse effects of repeated imaging (e.g., fasting, tail vein injections, anesthesia): group A was imaged on days 0, 3, 10, and 17, and group B was imaged on days 0, 1, 7, and 14.

PET images were reconstructed using an ordered subsets expectation maximization algorithm, and CT images were reconstructed using filtered back projection algorithm with a Shepp–Logan filter. Three-dimensional regions of interest for entire tumors (viable tumor plus necrotic core) were defined based on registered PET and CT images. Standard uptake values (SUV) for average and maximum uptake were calculated using the following formula:

$$SUV = \frac{Tumor\ FDG\ Concentration(\mu Ci/mL)}{Injected\ Dose\ (\mu Ci)/Body\ Weight(g)}$$

SUV data are displayed as a percentage of baseline. Maximum SUV (SUVmax) was compared for evaluation of viable tumor.

Statistical Analysis. All error bars shown are S.D. Two-tailed *t* tests were used to determine statistical significance as noted by $^*P < 0.05$; $^{**}P < 0.01$; and $^{***}P < 0.001$ in the figures.

Results

Tumor NADt Depletion Precedes ATP Depletion In Vivo. A novel isoindoline urea series of NAMPT inhibitors was identified in a screen for compounds that inhibited cell

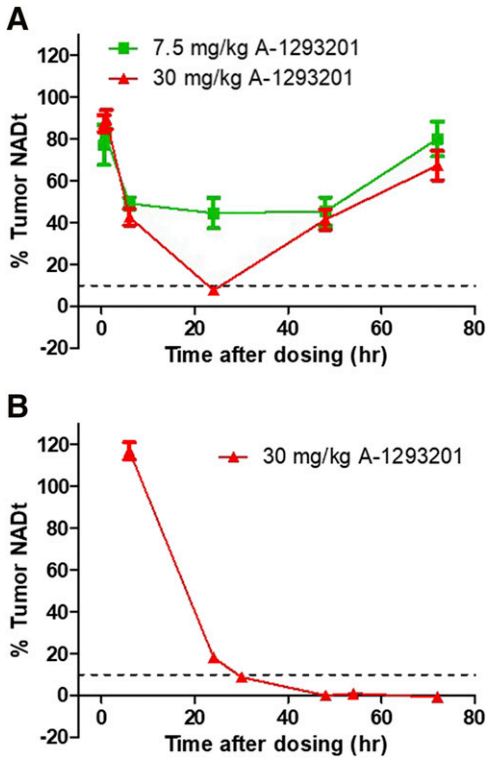

Fig. 1. NAD depletion in HCT116 xenografts. (A) Depletion of NADt in HCT116 xenografts following a single dose of either 7.5 (green) or 30 (red) mg/kg A-1293201. (B) Depletion of NADt in HCT116 xenografts following a multiple dose schedule of 30 mg/kg once per day for 3 days. Dashed line indicates 90% depletion of NADt. Data for both panels are expressed as percentage of tumor NADt in xenografts from mice that were not dosed with compound and are the average ± S.E.M. of four tumors/time point.

viability. A-1293201 and A-1326133 are lead compounds optimized from this series that are potent inhibitors of NAMPT. Inhibition of NAMPT by these compounds for at least 48 hours resulting in >90% depletion of NADt was required to elicit NADt depletion–dependent cytotoxicity (Wilsbacher et al., 2017).

To characterize the effects of different dosing schedules on the extent and duration of NAD^+/NADH depletion in a mouse xenograft model, NADt levels were measured in HCT116 tumors collected at various times following dosing with A-1293201. Following a single dose of A-1293201, tumor NADt was reduced relative to baseline at 6, 24, and 48 hours at both the 7.5 and 30 mg/kg dose levels (Fig. 1A). However, NADt levels were only decreased by >90% at 24 hours following the 30 mg/kg dose, and tumor NADt concentrations recovered to a little over 40% by 48 hours after dosing. Substantial reduction of NADt relative to baseline was not observed 72 hours following the single dose at either dose level. Relative to baseline, tumor NADt was decreased >90% at all time points after the second dose in the 30 mg/kg multiple dose schedule of A-1293201 (Fig. 1B).

To extend the analysis to ATP depletion, the kinetics of NAD and ATP depletion following A-1293201 treatment of HCT116 cells in culture was assessed. HCT116 cells were incubated with 0.1 and 1 μM A-1293201 in culture for 6, 24, 48, and 72 hours. At each time point, cells were harvested, and NADt and ATP levels relative to control cells were measured. For both compound concentrations, maximal depletion of ATP occurred at later time points postdrug addition than NADt depletion (Fig. 2A). Within 6 hours, NADt levels are reduced by 60% with no impact on ATP levels. However, at 24 hours after treatment initiation in vitro in HCT116 cells, NADt is completely depleted, with ATP levels reduced to 20% of control. ATP is fully depleted at 48 hours in HCT116 cells treated with either 0.1 or 1 μM A-1293201.

Expression levels of NAMPT have been shown to negatively correlate with potency of NAMPT inhibitors in cell viability assays (Xiao et al., 2013). We assessed NAMPT and NAPRT1 expression across a panel of cell lines and found that H460-LM cells express relatively high levels of NAMPT but do not express NAPRT1 (Supplemental Fig. 2). NADt and ATP levels were assessed following treatment of H460-LM cells with 0.1, 1, and 10 μM A-1293201 (Fig. 2B). The lowest A-1293201 dose decreased NADt levels in H460-LM cells, but did not result in complete NADt depletion and did not decrease ATP levels. In cells treated with 1 μM A-1293201, NADt levels were depleted about 95% after 24 hours, and ATP levels were partially depleted at 48 and 72 hours. NADt levels were depleted about 97% at 24 hours and completely depleted after 48 hours with the 10 μM A-1293201 dose. ATP levels were substantially depleted beginning at 48 hours and did not recover at 72 hours after dosing. Thus, the amount of drug and length of time needed to cause complete ATP depletion were higher for the H460-LM cell line than for HCT-116. These data confirm that ATP depletion is delayed relative to NADt

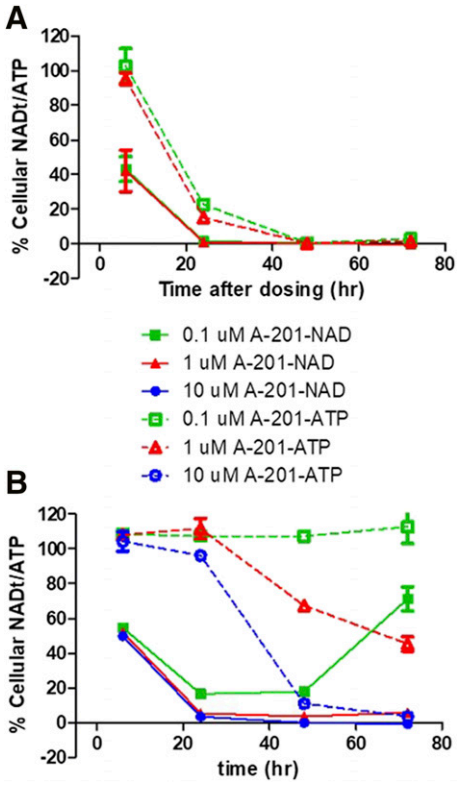

Fig. 2. NAD and ATP depletion in cultured cells. (A) Depletion of NADt (solid lines) and ATP (dashed lines) over time in HCT116 cells treated with 0.1 (green) or 1 (red) mM A-1293201. (B) Depletion of NADt (solid lines) and ATP (dashed lines) over time in H460-LM cells treated with 0.1 (green), 1 (red), or 10 (blue) mM A-1293201. Data for both panels are expressed as percentage of cellular NADt or ATP in cells treated with DMSO at each time point. Data are the average ± S.D. of duplicate samples and are representative of three independent experiments.

depletion. An expanded profiling of multiple cell lines confirmed the observation that higher concentrations of NAMPT inhibitor are needed to fully block NAMPT activity in cells with higher expression of NAMPT (see Supplemental Table 1).

Decreased Tumor FDG Uptake Related to ATP Depletion. In vivo imaging studies were carried out to determine what conditions were required to decrease tumor FDG uptake: 1) partial NAD^+ depletion, 2) full NAD^+ but only partial ATP depletion, or 3) full NAD^+ and full ATP depletion. To understand the impact of NAD^+ depletion on FDG uptake, we tested two doses of A-1293201, as follows: 7.5 mg/kg, which was shown to partially deplete NADt, and 30 mg/kg, which was shown to fully deplete NADt in vivo at 24 hours in HCT116 tumors (Fig. 1A). Multiple time points were evaluated to capture the relationship between NAD^+ and ATP depletion with tumor FDG uptake. Based on the pharmacodynamic data in Figs. 1 and 2A, NAD^+ levels are fully depleted with the 30 mg/kg dose at 24 hours, and ATP depletion should lag behind NAD^+ depletion. After the last dose in the 3-day treatment cycle in vivo, ATP levels are expected to be depleted because NAD^+ levels have been depleted for an extended period of time. A decrease in tumor FDG uptake was not observed with the 7.5 mg/kg dose at any time point (Fig. 3), despite a decrease in NAD^+ levels. There is no effect of subefficacious doses on targeting/imaging because that does not result in >90% inhibition of NAMPT/depletion of NAD in the tumor cells, which is required for ATP depletion and cell death. At the end of treatment during the first cycle, tumor FDG uptake was 121% ± 47% relative to baseline and not statistically different from the vehicle-treated group. With 30 mg/kg treatment, tumor FDG uptake was not significantly different from vehicle after 24 hours, but was 46% ± 23% of baseline tumor uptake at the end of the first treatment cycle. Just before the second treatment cycle, FDG uptake had recovered to near baseline values, but was again decreased to 49% ± 33% 24 hours after the last dose in the treatment cycle (Fig. 3). This pattern was repeated for the third treatment cycle (Fig. 3B).

Rescue of NADt Levels by NA Supplementation Is Reflected in the FDG Response in NAPRT-Proficient but Not NAPRT-Deficient Tumors. One potential method for mitigating on-target toxicity to normal tissues is to codose NA with the NAMPT inhibitor. Generation of NAD^+ from NA requires expression of NAPRT1, which is epigenetically regulated. Some cancers express NAPRT1 in addition to NAMPT, so codosing NA would result in NAD^+ production and may block the cytotoxic effects of NAMPT inhibitors when NA is used as a toxicity mitigation strategy (Duarte-Pereira et al., 2016). To determine whether generation of NAD^+ via the Preiss–Handler pathway would alter the effects of NAMPT inhibition on tumor FDG uptake, we treated animals bearing HCT116 tumors that express NAPRT1 (Supplemental Fig. 2) with A-1293201 plus NA. Codosing 30 mg/kg A-1293201 with 50 mg/kg NA resulted in similar tumor FDG uptake relative to vehicle and 50 mg/kg NA: 138% ± 33% relative to baseline after the last dose in the first cycle and 121% ± 36% after the last dose in the third cycle (Fig. 4, A and B). Treatment with A-1293201 alone in the same model resulted in a decrease in tumor FDG uptake relative to vehicle and A-1293201 codosed with NA, as seen in Fig. 4, A and B. Monotherapy with 30 mg/kg A-1293201 caused HCT116 xenograft growth inhibition, whereas codosing 30 mg/kg A-1293201 with NA did not (Fig. 4C). The extent of A-1293201 efficacy in this study correlated well with the compromised FDG uptake, indicating that FDG-PET can be used as a biomarker for NAD^+ and ATP depletion in tumors treated with NAMPT inhibitors.

To confirm that the attenuation of efficacy resulting from the addition of NA is dependent on NAPRT, a NAPRT-deficient xenograft model was evaluated. The ovarian cell model, A2780, does not express NAPRT1, and the antitumor activity of NAMPT inhibition cannot be rescued by NA addition in vitro (Supplemental Fig. 2; Supplemental Table 1). A-1326133, another lead NAMPT inhibitor, was dosed in mice bearing A2780 xenografts at 7.5 mg/kg in the absence and presence of 50 mg/kg NA. Tumor growth was inhibited to the same extent in both treatment groups (Fig. 5A), and this correlated with decreased FDG uptake (Fig. 5B). Tumor FDG uptake was decreased to 67% ± 21% of baseline tumor at the end of the first treatment cycle, and uptake remained decreased the day after the last dose of A-1326133 in each treatment cycle (Fig. 5B). Codosing the NAMPT inhibitor with 50 mg/kg NA had no effect on the decreased tumor FDG

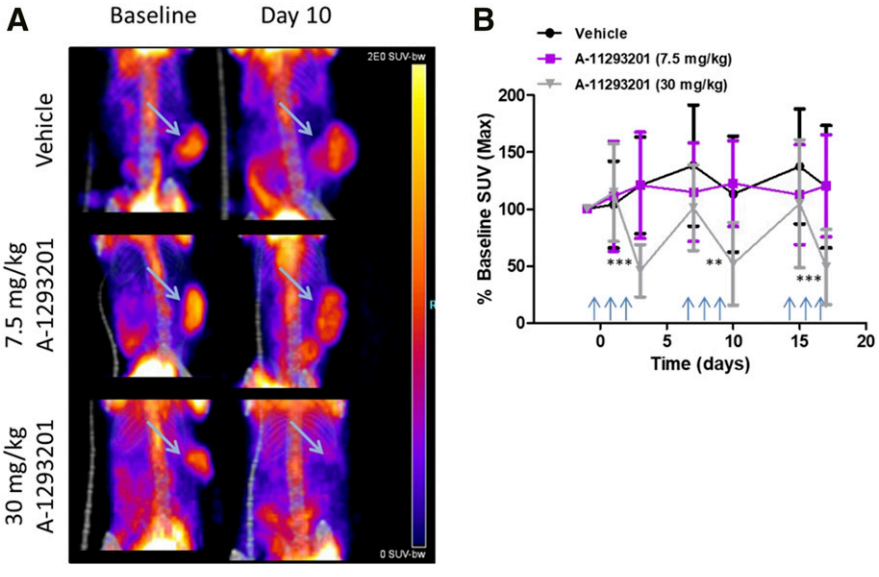

Fig. 3. FDG-PET in the HCT-116 xenograft model (NAPRT proficient). (A) Representative FDG-PET/CT images at baseline and day 10. Tumors are indicated by arrows. (B) Tumor FDG uptake as a percentage of baseline uptake based on maximum SUV. Treatment is indicated by arrows. Statistical significance relative to vehicle is indicated by stars (**P < 0.01 and ***P < 0.001).

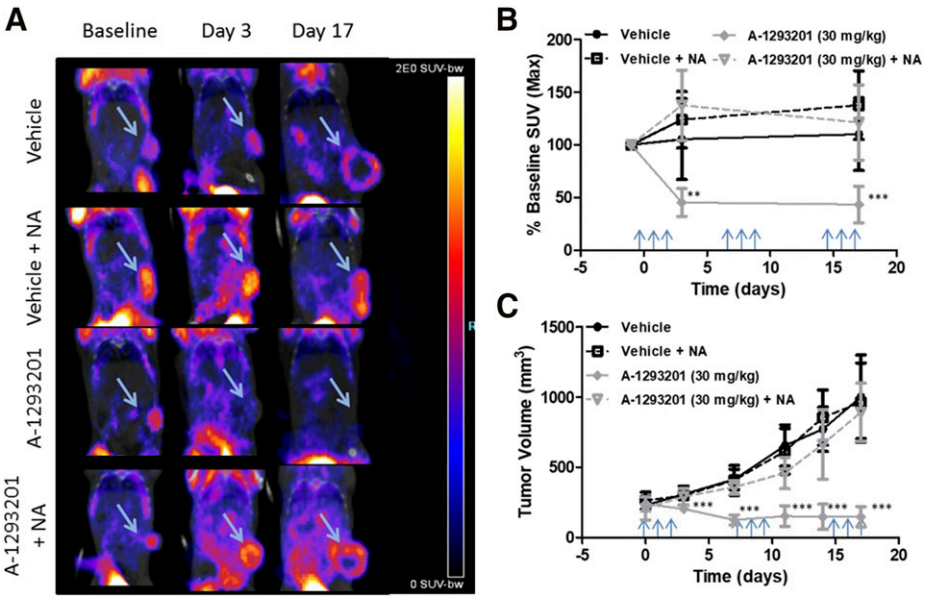

Fig. 4. FDG-PET in the HCT-116 xenograft model (NAPRT proficient) with NA codosing. (A) Representative FDG-PET/CT images at baseline, day 3, and day 10. Tumors are indicated by arrows. (B) Tumor FDG uptake as a percentage of baseline uptake based on maximum SUV. (C) Tumor volume during the course of treatment. Treatment days on the graphs are indicated by arrows. Statistical significance for each treatment relative to its control with or without NA is indicated by stars (**P < 0.01 and ***P < 0.001).

uptake in response to A-1326133 treatment, with FDG uptake at 58% ± 20% of baseline after the last dose in the first cycle with A-1326133 plus NA.

High NAMPT Expression Reduces Sensitivity to NAMPT Inhibition. Based on the in vitro results in Fig. 2B, a larger dose of a NAMPT inhibitor is needed to deplete NAD^+ and ATP levels in cells expressing higher levels of NAMPT. However, toxicity limits the dose of NAMPT inhibitors in vivo (Supplemental Table 2). For example, mice dosed with up to 45 mg/kg A-1326133 had no significant health issues. However, when mice were dosed with either 50 or 75 mg/kg, we observed 60% mortality and >20% bodyweight loss by day 5 of dosing. Codosing with NA protected against these animal health observations and allowed for higher dosing of the NAMPT inhibitor. When 75 mg/kg A-1326133 was codosed with 50 mg/kg NA, no significant animal health issues were observed. We treated animals with H460-LM tumors with either vehicle and NA, A-1326133 at a dose that would typically cause NAD^+ and ATP depletion in lower NAMPT-expressing models (15 mg/kg), or with NA and a dose level of the NAMPT inhibitor that would be toxic in the absence of NA (75 mg/kg). When 75 mg/kg A-1326133 and 50 mg/kg NA are codosed, tumor FDG uptake is 58 ± 19% relative to baseline after four doses, as seen in Fig. 6A, and is statistically different from the vehicle plus NA–treated group. The reduction in FDG uptake in the presence of 75 mg/kg A-1326133 plus NA corresponded to a significant tumor growth inhibition relative to the vehicle plus NA-treated group at 4 and 7 days. Conversely, no tumor growth inhibition was observed in the 15 mg/kg group, which corresponded with no observed decreases in tumor FDG uptake. Tumor FDG uptake increased to 116% ± 20% relative to baseline after four consecutive doses of 15 mg/kg A-1326133 and was not different from vehicle plus NA treatment. The average tumor volume in the 15 mg/kg A-1326133 group was also not decreased relative to the vehicle plus NA–treated group.

Discussion

In this study, we investigated the impact of dose, NA supplementation, and NAPRT and NAMPT expression status on tumor FDG uptake using PET imaging in mice. We found that ATP depletion lags behind NAD^+ depletion, decreases in tumor FDG uptake correspond with ATP depletion, and the ability of NA codosing to restore NADt levels in tumor-expressing NAPRT impacts efficacy in NAPRT-proficient, but not NAPRT-deficient tumors.

Depletion of NAD^+ following NAMPT inhibition results in blockade of glycolysis at the glyceraldehyde 3-phosphate dehydrogenase step. As a result of glyceraldehyde 3-phosphate dehydrogenase inhibition, there is a reduction in downstream metabolites, including pyruvate, which culminates in inhibition of the tricarboxylic acid cycle (Tan et al., 2013, 2015). The lack of NADH formation in the tricarboxylic acid cycle coupled with depletion of NAD^+ synthesis from nicotinamide by NAMPT prevents generation of ATP through oxidative phosphorylation. The timing of decreases in tumor FDG uptake in our studies suggests that ATP depletion is necessary to cause reduced cellular glucose uptake. A lag in ATP depletion was observed in in vitro studies, and the kinetics of the NAD^+ levels in vitro and in vivo is the same. Even at efficacious doses, tumor FDG levels are not decreased at 24 hours despite NAD^+ levels being substantially depleted. Reductions in tumor FDG uptake are observed after 3 days of dosing, when ATP is expected to be decreased. ATP is required to transport glucose into the cell and is involved in early phosphorylation steps. Because FDG has a fluorine atom in the 2′ position after phosphorylation instead of a hydroxyl group, it cannot undergo further metabolism. Therefore, FDG uptake can give insights into glucose transport and hexokinase activity, which are likely to be impacted by ATP depletion resulting from upstream NAMPT inhibition. Previously published in vitro data also demonstrate that NADt levels are depleted within 24 hours, ATP levels are depleted within 48 to 72 hours, and cell viability is decreased at 72 hours, suggesting that cytotoxicity occurs after ATP depletion (Wilsbacher et al., 2017).

Treatment of cancer cells in culture with NAMPT inhibitors was shown previously to cause sequential depletion of NAD^+ and ATP, followed by inhibition of glycolysis and cytotoxicity. A minimum of 90% inhibition of NAMPT for 48 hours

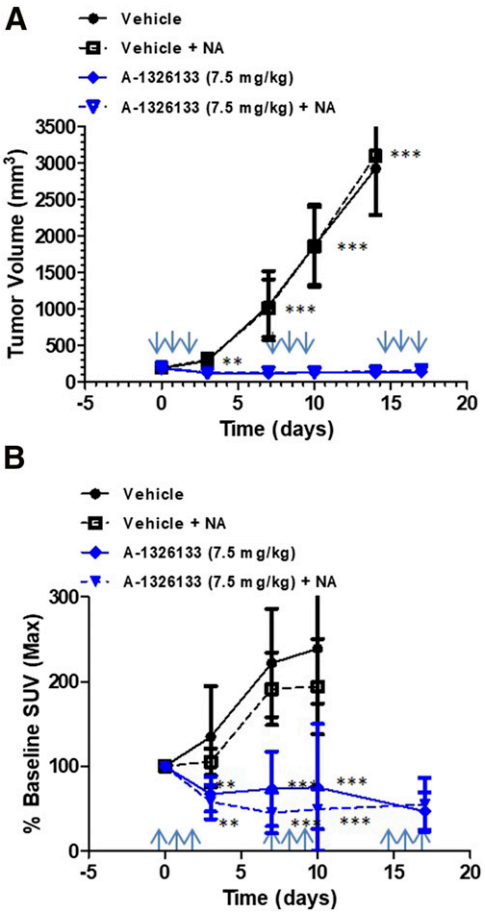

Fig. 5. FDG-PET in the A-2780 xenograft model (NAPRT deficient). (A) Tumor volume during the course of treatment with A-1326133 and/or NA. (B) Tumor FDG uptake as a percentage of baseline uptake based on maximum SUV. Statistical significance for each treatment relative to its control with or without NA is indicated by stars (**P < 0.01 and ***P < 0.001).

was necessary to observe maximal ATP depletion and result in cytotoxicity of HCT116 cells in vitro (Wilsbacher et al., 2017). In this study, we have shown that the same sequential depletion most likely occurs in vivo with >90% NADt depletion occurring about 24 hours after the first dose of A-1293201 in HCT116 xenografts, whereas inhibition of FDG uptake occurs later. Decreases in tumor FDG uptake are not observed at subefficacious doses of A-1293201 in HCT116 xenografts and A-1326133 in H460-LM xenografts, despite NAD^+ levels being depleted. This is most likely because NAD^+ is not depleted >90% for a sufficient period of time to result in maximal ATP depletion. In this study, inhibition of FDG uptake also correlated well with tumor growth inhibition, which makes FDG-PET a promising biomarker for NAMPT inhibitor target engagement in vivo.

Previous studies have reported decreases in tumor FDG uptake with the NAMPT inhibitors, FK866 and GMX1777 (Kato et al., 2010; Jensen et al., 2013). FK866 and GMX1778, the prodrug of GMX1777, have similar potencies as A-1326133 (Supplemental Table 3). Because different xenograft models were used and it is unclear whether the drug exposures between the studies are similar, it is difficult to directly compare the magnitude of the changes. Although the timing of NAD^+ and ATP depletion should be similar regardless of NAMPT inhibitor, the timing of imaging relative to drug treatment used in the previous studies could be contributing to the differences in the amount of tumor FDG uptake, which should occur when ATP is maximally depleted, that is observed.

Our studies add additional insight into the pharmacologic effects of NAMPT inhibition in the tumor, including the influence of NAMPT and NAPRT1 expression and NA coadministration on sensitivity to NAMPT inhibition as measured by tumor FDG uptake. Codosing NA with NAMPT inhibitor treatment may be a viable strategy for mitigating NAMPT inhibitor toxicity by providing an alternate route of NAD^+ synthesis in normal tissues that express NAPRT1. However, this strategy is feasible only in subjects with NAPRT1-negative tumors. Imaging could also confirm that an appropriate patient population is being treated and provide insight into lesion-to-lesion heterogeneity. Lesions with low to moderate NAMPT expression and no NAPRT1 expression, if NA is codosed, are most likely to respond. If a mixture of NAMPT and NAPRT1 expression is present, a heterogeneous response should be observed by FDG-PET. Codosing with NA may also allow for more efficacious treatment in tumors with high NAMPT expression. In our study in the H460-LM model, a high dose of the NAMPT inhibitor that would be toxic to normal tissue without NA supplementation could be administered, and it resulted in decreased FDG uptake and a corresponding reduction in tumor volume even though expression of NAMPT was high.

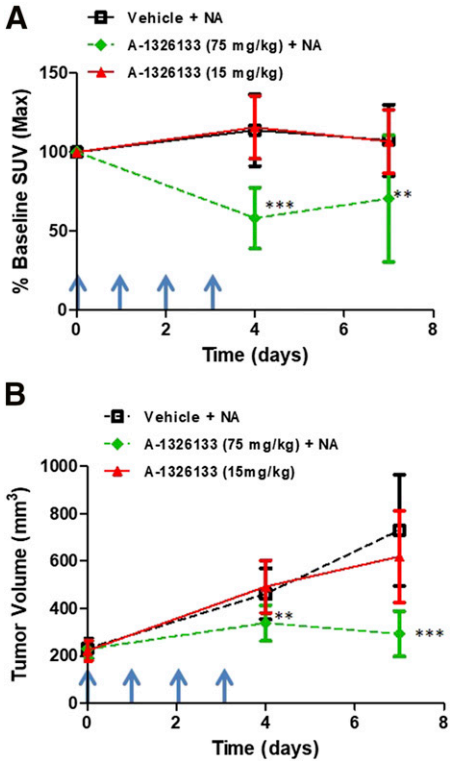

Fig. 6. FDG-PET in the H460 LM xenograft model (NAPRT deficient). (A) Tumor FDG uptake as a percentage of baseline uptake based on maximum SUV. (B) Tumor volume during the course of treatment. Treatment is indicated by arrows. Statistical significance relative to vehicle is indicated by stars (**P < 0.01 and ***P < 0.001).

In conclusion, our imaging data suggest that tumor FDG uptake can provide insight into the ATP status inside the tumor after NAMPT therapy. Such an approach could be used clinically as a pharmacodynamic biomarker to help understand the implications of dose, schedule, rescue strategy, or other clinical biomarkers.

Authorship Contributions

Participated in research design: Buchanan, Gao, Mudd, Tse, Voorbach, Wilsbacher.

Conducted experiments: D. Cheng, M. Cheng, Guo, Wilsbacher, Voorbach.

Performed data analysis: D. Cheng, M. Cheng, Guo, Mudd, Voorbach, Wilsbacher.

Wrote or contributed to the writing of the manuscript: Buchanan, Mudd, Tse, Wilsbacher.

References

Burgos ES (2011) NAMPT in regulated NAD biosynthesis and its pivotal role in human metabolism. *Curr Med Chem* **18**:1947–1961.

Chiarugi A, Dölle C, Felici R, and Ziegler M (2012) The NAD metabolome--a key determinant of cancer cell biology. *Nat Rev Cancer* **12**:741–752.

Duarte-Pereira S, Pereira-Castro I, Silva SS, Correia MG, Neto C, da Costa LT, Amorim A, and Silva RM (2016) Extensive regulation of nicotinate phosphoribosyltransferase (NAPRT) expression in human tissues and tumors. *Oncotarget* **7**: 1973–1983.

Gupte R, Liu Z, and Kraus WL (2017) PARPs and ADP-ribosylation: recent advances linking molecular functions to biological outcomes. *Genes Dev* **31**:101–126.

Imai S (2009) Nicotinamide phosphoribosyltransferase (Nampt): a link between NAD biology, metabolism, and diseases. *Curr Pharm Des* **15**:20–28.

Jensen MM, Erichsen KD, Johnbeck CB, Björkling F, Madsen J, Bzorek M, Jensen PB, Højgaard L, Sehested M, and Kjær A (2013) [18F]FLT and [18F]FDG PET for non-invasive treatment monitoring of the nicotinamide phosphoribosyltransferase inhibitor APO866 in human xenografts. *PLoS One* **8**:e53410.

Kato H, Ito E, Shi W, Alajez NM, Yue S, Lee C, Chan N, Bhogal N, Coackley CL, Vines D, et al. (2010) Efficacy of combining GMX1777 with radiation therapy for human head and neck carcinoma. *Clin Cancer Res* **16**:898–911.

Preiss J and Handler P (1958) Biosynthesis of diphosphopyridine nucleotide. II. Enzymatic aspects. *J Biol Chem* **233**:493–500.

Sampath D, Zabka TS, Misner DL, O'Brien T, and Dragovich PS (2015) Inhibition of nicotinamide phosphoribosyltransferase (NAMPT) as a therapeutic strategy in cancer. *Pharmacol Ther* **151**:16–31.

Shames DS, Elkins K, Walter K, Holcomb T, Du P, Mohl D, Xiao Y, Pham T, Haverty PM, Liederer B, et al. (2013) Loss of NAPRT1 expression by tumor-specific promoter methylation provides a novel predictive biomarker for NAMPT inhibitors. *Clin Cancer Res* **19**:6912–6923.

Tan B, Dong S, Shepard RL, Kays L, Roth KD, Geeganage S, Kuo MS, and Zhao G (2015) Inhibition of nicotinamide phosphoribosyltransferase (NAMPT), an enzyme essential for NAD+ biosynthesis, leads to altered carbohydrate metabolism in cancer cells. *J Biol Chem* **290**:15812–15824.

Tan B, Young DA, Lu ZH, Wang T, Meier TI, Shepard RL, Roth K, Zhai Y, Huss K, Kuo MS, et al. (2013) Pharmacological inhibition of nicotinamide phosphoribosyltransferase (NAMPT), an enzyme essential for NAD+ biosynthesis, in human cancer cells: metabolic basis and potential clinical implications. *J Biol Chem* **288**: 3500–3511.

Wilsbacher JL, Cheng M, Cheng D, Trammell SAJ, Shi Y, Guo J, Koeniger SL, Kovar PJ, He Y, Selvaraju S, et al. (2017) Discovery and characterization of novel non-substrate and substrate NAMPT inhibitors. *Mol Cancer Ther* **16**:1236–1245.

Xiao Y, Elkins K, Durieux JK, Lee L, Oeh J, Yang LX, Liang X, DelNagro C, Tremayne J, Kwong M, et al. (2013) Dependence of tumor cell lines and patient-derived tumors on the NAD salvage pathway renders them sensitive to NAMPT inhibition with GNE-618. *Neoplasia* **15**:1151–1160.

Address correspondence to: Dr. Sarah R. Mudd, AbbVie, 1 North Waukegan Rd, North Chicago, IL 60064. E-mail: sarah.mudd@abbvie.com